

CrossMark
click for updatesCite this: *J. Mater. Chem. C*, 2014, 2, 7029

H-bonded complexes containing 1,3,4-oxadiazole derivatives: mesomorphic behaviour, photophysical properties and chiral photoinduction†

André A. Vieira,^a Emma Cavero,^b Pilar Romero,^c Hugo Gallardo,^{*a} José Luis Serrano^b and Teresa Sierra^{*c}

Two series of new V-shaped acids derived from 1,3,4-oxadiazoles are described. These acids were used to prepare supramolecular complexes through hydrogen bonding with 2,4-diamino-6-dodecylamino-1,3,5-triazine in a 3 : 1 ratio, respectively. The formation of the complexes was studied by infrared and NMR techniques. The thermal behaviour and mesomorphic properties of all the complexes were investigated by polarized light optical microscopy, differential scanning calorimetry and X-ray diffraction. Hexagonal and rectangular columnar mesophases were observed for all complexes at room temperature, without evidence of crystallization. The results of circular dichroism studies allowed us to propose that in the liquid crystalline state these materials adopt a helical columnar organization and this chirality can be controlled by irradiation with CPL. Furthermore, the complexes display strong blue luminescence in solution and in the mesophase.

Received 30th April 2014
Accepted 25th June 2014

DOI: 10.1039/c4tc00886c

www.rsc.org/MaterialsC

Introduction

Self-organized structures based on liquid crystals have great potential for the implementation of functional soft materials due to the combination of unique features such as molecular order and mobility.¹ In particular, columnar liquid crystals offer myriad possibilities for molecular design and a high level of structural control to attain well defined 1D organization, with an additional two-dimensional order of the columns.² Furthermore, the use of non-covalent interactions to stabilize columnar arrangements may lead to highly consistent materials through rather simple synthesis and purification procedures, in which the supramolecular organization remains stable at room temperature appropriate for applications. In particular, π -stacking and hydrogen-bonding allow the construction of well-defined columnar arrangements in an easy, dynamic and reproducible way.³

In a further step, columnar liquid crystals provide the basis to achieve helical supramolecular architectures that allow the

expression of supramolecular chirality in functional materials.⁴ On one hand, the higher level of order associated with a helical disposition of the molecules along the column can give rise to an improvement in the anisotropic properties, pointing to the application of these materials as semiconductors, photoconductors, organic light emitting diodes and photovoltaic cells.^{2,4,5} On the other hand, supramolecular chirality can be achieved and/or controlled by tailoring the molecular structure (chiral information encoded in the constituent molecules),⁶ intermolecular interactions (*i.e.* hydrogen bonding, π -stacking, *etc.*)⁷ or an external source such as light.⁸

We have already demonstrated the versatility of the supramolecular system based on 2-alkylamino-4,6-diamino-1,3,5-triazine and V-shaped acids to obtain functional columnar liquid crystals with well-defined columnar organization. These structures arise due to the synergistic action of the π -stacking tendency of the melamine-derived core and the strong lateral interactions between V-shaped molecules. In these materials an inherent helical architecture is proposed and this arises from the propeller-like conformation of the complex.⁹ On the basis of this helical architecture supramolecular chirality is achieved in functional self-organized materials. Firstly, chiral information present in the stereogenic centres of peripheral hydrocarbon tails is transmitted to the columnar architecture and supramolecular optical activity in the mesophase is detected by CD spectroscopy.^{10,11} Secondly, the incorporation of the 2,5-diphenyl-1,3,4-oxadiazole moiety into the V-shaped acid provided luminescent columnar liquid crystals with helical

^aDepartamento de Química, INCT-Catálise, Universidade Federal de Santa Catarina – UFSC, 88040-900 Florianópolis-SC, Brazil. E-mail: hugo@qmc.ufsc.br; Tel: +55 48 37219544

^bDepartamento de Química Orgánica, Facultad de Ciencias, Institute of Nanoscience of Aragon (INA), Universidad de Zaragoza, C/Pedro Cerbuna 12, 50009-Zaragoza, Spain
^cInstituto de Ciencia de Materiales de Aragón, Dep. Química Orgánica, Facultad de Ciencias, Universidad de Zaragoza – CSIC, C/Pedro Cerbuna 12, 50009 Zaragoza, Spain. E-mail: tsierra@unizar.es; Tel: +34 976 762276

† Electronic supplementary information (ESI) available. See DOI: 10.1039/c4tc00886c

architectures, which in turn led to supramolecular activity when chiral tails were present in the V-shaped acid.¹⁰ Additionally, photoresponsive features established by the ability of the azobenzene-derived systems to follow the helicity of circular polarized light¹¹ have been verified in these materials.

As a continuation of this research, we describe here the synthesis and characterization of novel luminescent V-shaped acids derived from 2,5-diphenyl-1,3,4-oxadiazole, and their corresponding H-bonded complexes with 2,4-diamino-6-dodecylamino-1,3,5-triazine in a 3 : 1 ratio, respectively. Two series of complexes were prepared and they differ in the structure of the V-shaped acid, namely a symmetrical (containing oxadiazole groups in both arms) and an unsymmetrical one (bearing an oxadiazole group (X) in one arm and an azobenzene group (A) on the other). As in previous studies, these complexes have a non-discotic structure that favours columnar mesomorphism with helical superstructures. Furthermore, the presence of oxadiazole promotes luminescent properties in the building blocks and this is transmitted to the bulk. Chirality in the peripheral tails leads to helical superstructures that are biased towards optically active materials by the transfer of molecular chirality to the supramolecular organization. The presence of azobenzene groups allows the control of chirality using circularly polarized light as an external chiral stimulus. The combination of these properties should lead to multifunctional self-organized materials with defined supramolecular architectures.

Results and discussion

Synthesis

The melamine **M**, 2,4-diamino-6-dodecylamino-1,3,5-triazine, was prepared by the reaction of dodecylamine with 2,4-diamino-6-chloro-1,3,5-triazine using sodium hydrogen carbonate as a base.¹²

The V-shaped acids **X(S)10*X(S)10***, **X(R)10*X(R)10***, **X12X12**, **X(S)10*A(S)10***, **X(S)10*A12**, **X12A(S)10*** and **X12A12** were prepared following the synthesis pathway outlined in Schemes 1 and 2.

The starting materials in the synthesis route were the O-alkylbenzonitriles **1**, which were used to obtain the respective

tetrazoleheterocycles **2** by Huisgen¹³ 1,3-dipolar cycloaddition using sodium azide and ammonium chloride in DMF. The tetrazole compounds **2** were reacted with freshly prepared methyl 4-(chlorocarbonyl)benzoate in pyridine to afford the 3,5-disubstituted 1,3,4-oxadiazole¹⁴ **4** in good yields (68–93%). The carbonyl group in the *para* position with respect to the tetrazole ring probably inhibits the progress of this reaction. The acid intermediates **5** were obtained in quantitative yield by hydrolysis of the ester function of compound **4** with potassium hydroxide in ethanol/water. Compounds **7** were obtained by diesterification of triisopropylsilyl 3,5-dihydroxybenzoate (**6**) with the respective acid **3** using *N,N'*-dicyclohexylcarbodiimide (DCC) and 4-(*N,N*-dimethylamino)pyridinium 4-toluenesulfonate (DPTS) in dichloromethane (Scheme 2).

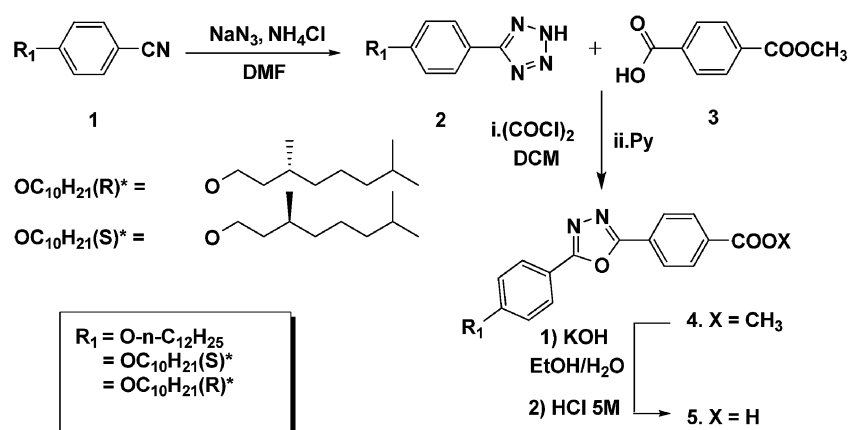
The desired final acids **8 (XX)** were obtained in good yields (74–97%) by removal of the triisopropylsilyl group with tetra-*n*-butylammonium fluoride in dichloromethane (see ESI†). The acids **11 (XA)** were obtained by the esterification of the corresponding phenol **9** bearing the azo group, which was reported previously,^{11a} with acid **5** and subsequent removal of the triisopropylsilyl group.

The structures and purities of compounds **XX** and **XA** were fully characterized and verified by ¹H and ¹³C NMR spectroscopy, elemental analysis, and MALDI-TOF mass spectrometry (see ESI†).

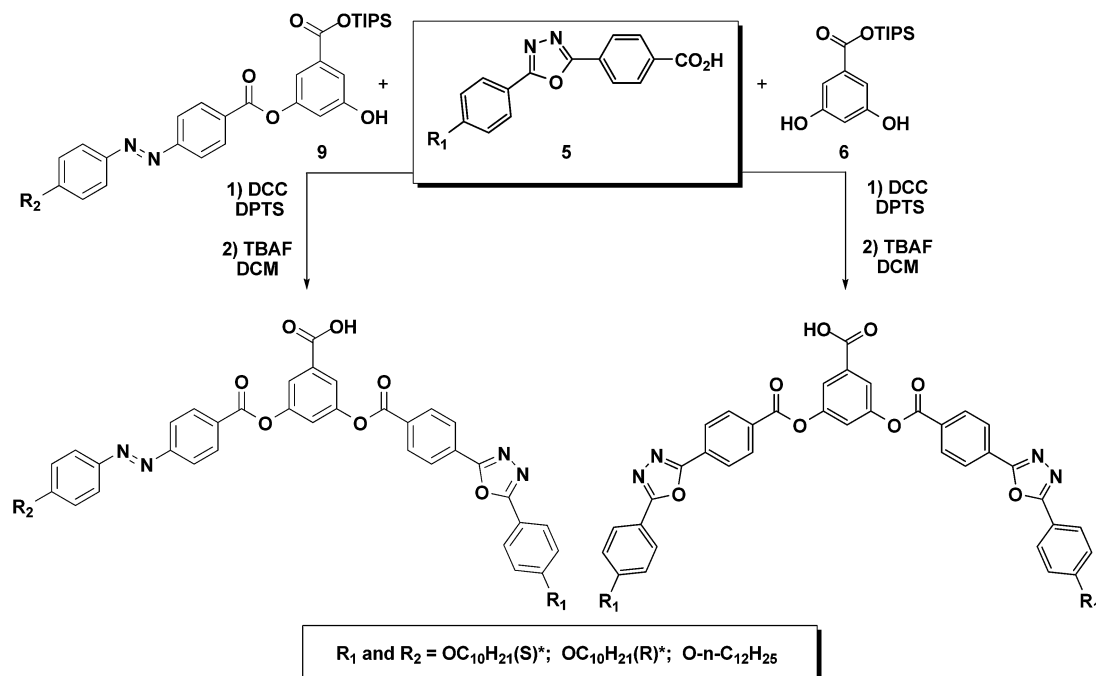
After the preparation and characterization of the final acids (**XX** and **XA**) and the melamine (**M**), the complexes **M-XX** and **M-XA** were prepared by dissolving both compounds in tetrahydrofuran (Scheme 3) in a proportion of 1 mole of melamine to 3 moles of acid. The solvent was evaporated by stirring the mixture at 40 °C, on a rotary evaporator, to prevent precipitation of the acid.

The formation of the complexes **M-XX** and **M-XA** was studied by IR and NMR (see ESI†). The IR spectra (Fig. S1†) showed differences between the acids **XX** and **XA** and their complexes **M-XX** and **M-XA**, especially in regions corresponding to the carbonyl, O–H and N–H groups responsible for the interactions between molecules.

All of the ¹H NMR spectra (Fig. 1–3 and S3–S10†) clearly indicate the formation of complexes, where it is assumed that



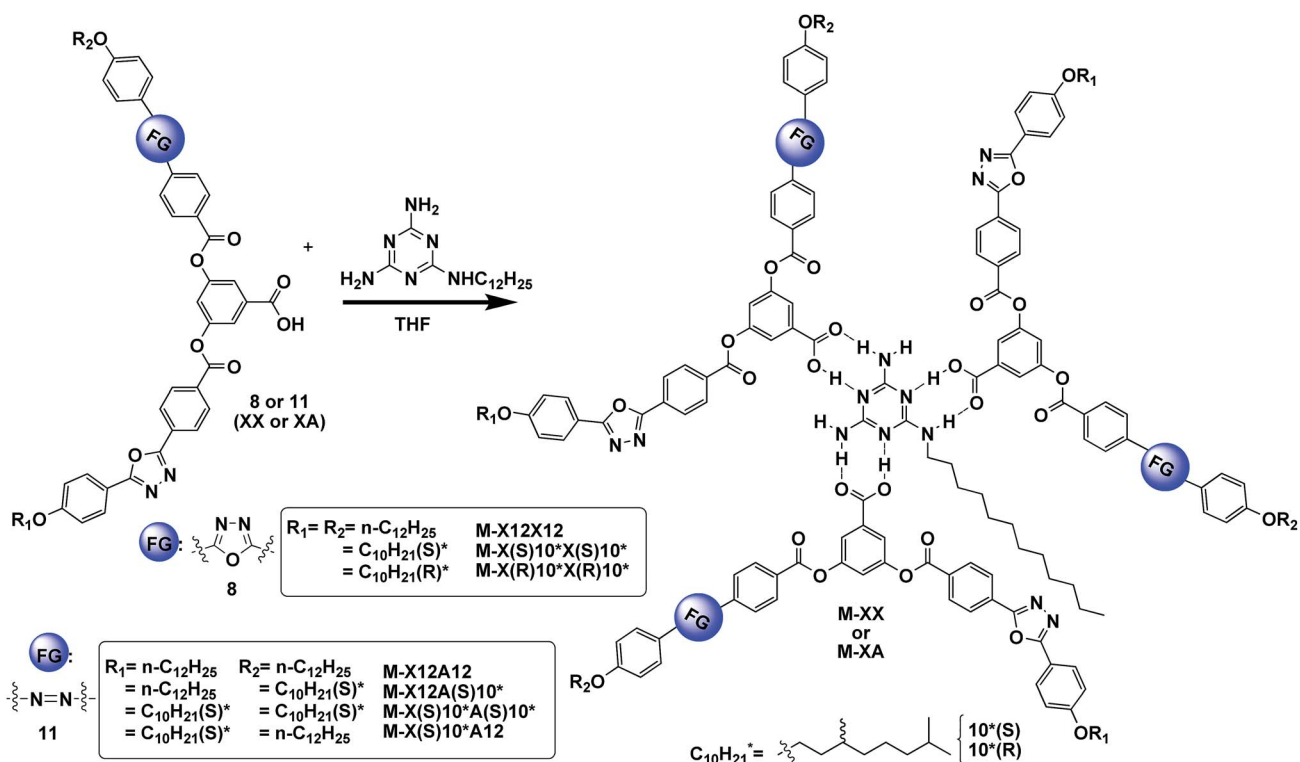
Scheme 1 Synthesis route of the intermediate acids **5**.



Scheme 2 Synthesis of the final acids 8 and 11 (XX and XA).

there is a rapid equilibrium between the complex and its components.⁹ Large displacements were observed for the chemical shifts of the five NH groups of **M**. The downfield shifts of these hydrogen atoms can be seen in Fig. 1: 4.92 and 4.81 ppm before the complexation and 6.79, 6.46 and 5–7 ppm (very

broadband) after formation of the supramolecular complex **M-X(S)10*X(S)10*** in CD_2Cl_2 . The protons of the *N*-methylene group of the alkyl chain in the triazine are slightly deshielded, while the proton of the central benzene ring *para* to the carboxylic acid group is shifted upfield.

Scheme 3 General preparation of the complexes **M-XX** and **M-XA** from 3 moles of acid (**XX** and **XA**) and 1 mole of triazine (**M**).

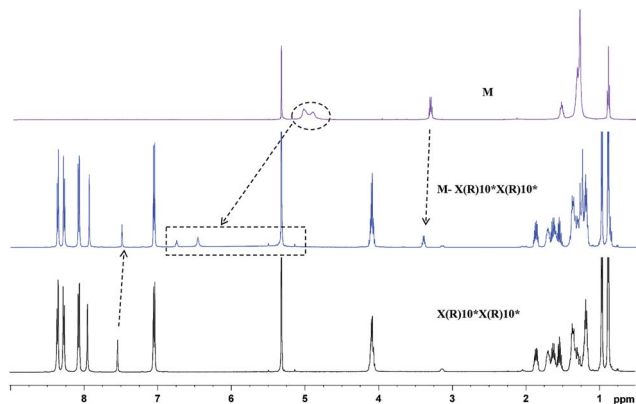


Fig. 1 Protons of the melamine, the methylene of the alkyl chain of the melamine and the hydrogen of the central aromatic ring of the acid $X(S)10^*X(S)10^*$ are displaced after formation of the complex (500 MHz, CD_2Cl_2 , 25 °C).

Likewise, variations in the chemical shifts of the ^{13}C signals of carbon atoms involved in the formation of the supramolecular structure were also clearly observed (Fig. 2). The ^{13}C signals of the triazine core (167.5, 166.8, 166.5 ppm) were shifted to lower frequencies by 4 or 5 ppm (162.8, 160.9, 159.9 ppm, respectively) and the ^{13}C signals of the carboxylic acid (Z) and of the aromatic central ring (M, N, O, P) were shifted markedly after complexation.

Additional experiments to study the formation of these complexes in solution were performed. Diffusion ordered spectroscopy (DOSY) revealed a unique diffusion coefficient for the complexes that was different from those of the acid and melamine (Fig. S3–S5[†]). Moreover, we previously reported similar systems and showed that the stoichiometry of these complexes in solution is 1 : 1.¹⁵ In this present work, the continuous variation method was applied to 1H NMR experiments on the complex $M-X(S)10^*X(S)10^*$. Titration experiments in solution in CD_2Cl_2 and THF-d8 showed that all NH proton signals and the N-CH₂ signals of the alkyl chain of the melamine **M**, as well as the hydrogen atoms of the central aromatic ring of the acid $X(S)10^*X(S)10^*$, were displaced upon increasing the proportion of acid in the solution while keeping the melamine concentration constant. Binding constants of

$615 \pm 18 \text{ L mol}^{-1}$ in CD_2Cl_2 and $161 \pm 8 \text{ L mol}^{-1}$ in THF-d8 were calculated by nonlinear curve fitting of the chemical shifts.

The stoichiometry, however, became 3 : 1 in the bulk material when the molar amount of the acid was three times that of the melamine. The ^{13}C CPMAS spectra of solid samples helped to confirm the complex stoichiometry (Fig. 3). The shielding of the carboxylic acid carbon in the solid spectrum of the complex, in contrast to that observed in solution (Fig. 2), can be attributed to π stacking of the central aromatic core.

Thermal properties

All of the acids **XX** and **XA** and final complexes **M-XX** and **M-XA** were investigated by polarized optical microscopy (POM) and differential scanning calorimetry (DSC) in order to determine their thermal and thermodynamic properties and mesomorphism. None of the acids used to form these complexes are liquid crystalline (see ESI[†]). The investigation of the thermal stability of these new V-shaped acids by thermogravimetric analysis (TGA) indicated that they did not exhibit weight loss at temperatures below 290 °C under a nitrogen atmosphere. The transition temperatures and enthalpy values of the complexes are given in Table 1.

When observed under the optical microscope, all the complexes appear as homogenous samples, and a uniform texture develops on cooling from the isotropic liquid in all cases. This and the appearance of a sharp peak in the cooling DSC scan (see ESI[†]), corresponding to the transition I-mesophase, support the correct formation of the acid-melamine complexes. The mesophases give in all cases poorly defined textures between crossed polarizers such as those shown in Fig. 4 and the ESI.[†] Nevertheless, these textures are reminiscent of those observed for previously described propeller-like complexes which are structurally related. A slight difference in textures between complexes containing acids **XX** and complexes containing acids **XA** was detected. For the former, homeotropic zones appeared on cooling and this indicated a uniaxial columnar arrangement such as in the hexagonal columnar

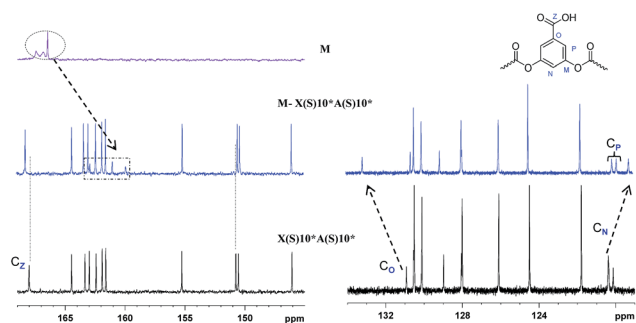


Fig. 2 Main shifts in ^{13}C NMR spectra after formation of the complex $M-X(S)10^*A(S)10^*$ (125 MHz, CD_2Cl_2 , 25 °C).

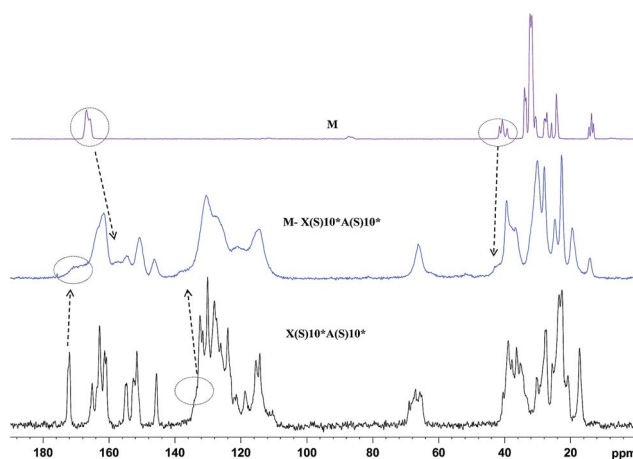


Fig. 3 ^{13}C -CPMAS spectra of acid $X(S)10^*A(S)10^*$ (bottom), $M-X(S)10^*A(S)10^*$ complex (middle) and **M** triazine (top).

Table 1 Thermal properties and lattice parameters of the complexes M-XX and M-XA

Complexes	Phase	Temp. ^a (°C)	ΔH [kJ mol ⁻¹]	Phase	Temp. ^a (°C)	Phase	Parameter lattice ^b (Å)
M-X(S)10*X(S)10*	I	147.6	12.8	Col _h	87.9	g	$a = 50.2$ $h = 3.4$
M-X(R)10*X(R)10*	I	149.1	19.4	Col _h	87.9	g	$a = 49.7$ $h = 3.4$
M-X12X12	I	181.4	42.9	Col _h	92.2	g	$a = 47.5$ $h = 3.5$
M-X(S)10*A(S)10*	I	93.3	5.8	Col _r			$a = 96.1$ $b = 70.4$
M-X(S)10*A12	I	107.0	10.0	Col _r			$a = 82.2$ $b = 78.6$
M-X12A(S)10*	I	113.9	14.8	Col _r			$a = 78.6$ $b = 77.0$
M-X12A12	I	119.5	16.0	Col _r			$a = 98.6$ $b = 78.9$

^a Transition temperatures were determined by DSC on the second cooling scan at 10 °C min⁻¹. I = isotropic liquid; Col_h = hexagonal columnar mesophase; Col_r = rectangular columnar mesophase. ^b All X-ray diffraction experiments were carried out at room temperature.

mesophase (Fig. 4a and S11†). This feature was not observed for the latter compound (Fig. 4b and S11†), which displayed textures similar to those observed for previously described rectangular columnar mesomorphic complexes.¹¹ In any case, the type of two-dimensional arrangement was further confirmed by X-ray diffraction (see below).

All of the complexes formed by the melamine derivative, **M**, and the acids **XX** and **XA** appeared as homogenous materials and showed liquid crystalline behaviour, with wide mesophase temperature ranges. This finding also supports the formation of H-bonded complexes since the V-shaped acids were not mesogenic (see ESI†). According to the thermograms registered by DSC, the mesophase remained stable until room temperature, without crystallization (after slow cooling from the isotropic state), for complexes containing unsymmetric acids **XA**. Complexes derived from symmetric acids **XX** show a glass transition at around 90 °C, and this signifies that the mesophase is frozen in a glassy state. This behavior reflects the strength of the hydrogen bonding interactions between the acid and melamine and is consistent with previously published studies.^{9–11,15,16}

The complexes formed with **XX** acids show higher clearing temperatures than the complexes formed with **XA** acids, and this is probably due to the symmetric structure of the acid, in

the presence of two 2,5-diphenyl-1,3,4-oxadiazole arms, which promotes stronger intermolecular interactions.

Branched chains derived from citronellol, in **M-X(S)10*X(S)10*** and **M-X(R)10*X(R)10***, led to a decrease of ca. 30 °C in the clearing temperatures with respect to their achiral homologue **M-X12X12** with linear chains.

Likewise, a decrease in the clearing temperatures was also observed for the **M-XA** complexes bearing branched chains (**M-X(S)10*A(S)10***, **M-X(S)10*A12**, and **M-X12A(S)10***) compared with their linear analogue **M-X12A12**, with the decreases ranging from 12.5–26 °C and the difference being more pronounced when both tails in the acid were derived from citronellol.

Structural characterization of the mesophase

The mesophases of the complexes **M-XX** and **M-XA** were studied and their parameters were measured by X-ray diffraction at room temperature (Tables 1 and S1†). As mentioned above, these materials did not crystallize on slow cooling. Accordingly, for all the complexes, X-ray experiments were carried out on samples slowly cooled from the isotropic liquid, so that the mesophase could develop completely.

The reflections observed in the small-angle X-ray scattering (SAXS) patterns obtained for the complexes **M-XX** were consistent with a hexagonal columnar (Col_h) mesophase (Table S1†). The SAXS patterns of **M-X(S)10*X(S)10*** (Fig. 5a) and **M-X(R)10*X(R)10*** showed a set of three low-angle sharp maxima with a reciprocal spacing ratio 1 : $\sqrt{3}$: $\sqrt{7}$ and the patterns of **M-X12X12** contained a set of two low-angle sharp maxima with a reciprocal spacing ratio 1 : 2. With the respective absence of the reflection (20) and the reflection (11),¹⁷ these maxima can be assigned to the (10), (11), (21) and (10), (20) reflections, respectively, of a two-dimensional hexagonal lattice. In the wide-angle X-ray scattering (WAXS) patterns, two diffuse maxima were observed for all complexes (Fig. S13†). The inner maximum corresponds to the conformationally disordered

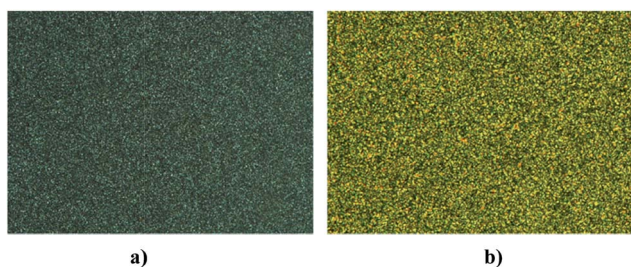


Fig. 4 Polarized optical photomicrographs taken at room temperature for (a) **M-X12X12** and (b) **M-X12A(S)10***.

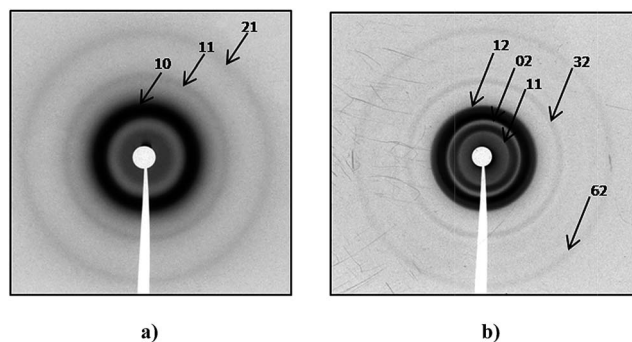


Fig. 5 SAXS diagram of the mesophase of $M-X(S)10^*X(S)10^*$ (a) and $M-X12A(S)10^*$ (b).

aliphatic chain and is, usually observed in liquid-crystalline compounds. The outer maximum observed at 3.4 Å and 3.5 Å, respectively, confirms the long range correlation order of the columnar mesophase and represents the mean stacking distance between the molecular cores along the column (h parameter of the Col_h mesophase).

From the values of the stacking parameter (h) it was possible to determine the number of complexes per unit cell (Z). Considering a density close to 0.85 g cm^{-3} , which is a reasonable value for organic materials of this type, the Z value is 1 for all the three complexes, which means that there is one complex per columnar stratum.⁹

The reflections observed in the SAXS patterns obtained for all complexes **M-XA** were consistent with rectangular columnar (Col_r) mesophases (Table S1†). As an example, a set of five maxima was observed for $M-X12A(S)10^*$ (Fig. 5b). These maxima can be assigned to the (11), (02), (12), (32) and (62) reflections of the two-dimensional rectangular lattice. For all the complexes, odd-values can be obtained for $h + k$ ruling out the $C2mm$ symmetry, and this is consistent with a $P2gg$ symmetry for the rectangular lattice. WAXS patterns showed the diffuse maximum corresponding to the disordered aliphatic tails, but a second high angle halo was absent for all of the materials, meaning that the correlation along the column in the mesophase is only short range and there is no regular stacking distance. Nevertheless, on the basis of our previous studies, and assuming densities of around $0.85\text{--}0.9 \text{ g cm}^{-3}$, the stacking distances along the column can be estimated between 3.3 and 3.85 Å, and this allows us to estimate the number of complexes per unit cell (Z). The Z values obtained are 4, which indicate two molecules per column, and this is consistent with values obtained for similar systems described previously.^{9,10,11c}

Chiroptical properties

It has been proposed in previous studies that this type of mesogen, consisting of a melamine derivative surrounded by three V-shaped acids, can adopt a propeller-like conformation that yields columnar architectures with inherent helical organization. The helical sense can be controlled by the presence of chiral tails in the acid partner and can be detected by circular dichroism measurements in the mesophase.⁹ Moreover, the

presence of azobenzene in the V-shaped acids confers on the complex the ability to respond to light as an external stimulus. Indeed, the photoinduced E/Z isomerization of azobenzene is a well-documented phenomenon, which proceeds reversibly upon irradiation with UV and visible light.¹⁸ When this process is driven by circularly polarized light (CPL), chirality can be induced into liquid crystalline organization.^{8,19} This phenomenon has been described for calamitic and B-type liquid crystalline organization, whereas, for columnar mesophases, it is still limited to the present type of propeller-like complexes.

The optical activity of the mesophase was studied for all of the chiral complexes by Circular Dichroism (CD) on thin films (ca. 300 nm to 1 mm thickness measured by profilometry) prepared by casting a dichloromethane solution of the corresponding complex onto an amorphous quartz plate and subsequent thermal treatment as for X-ray experiments. For every complex, six CD spectra were recorded at six different orientations measured by rotating the sample cells by 60° around the light beam. The spectra were almost identical for all orientations of the sample, and this rules out the prevalence in the observed signals of possible linear dichroism effects due to the macroscopic orientation.²⁰

The study of the chiroptical properties of these materials had two objectives. First, it was planned to determine whether the chirality of the chiral tails is transmitted to the supramolecular organization of the mesophase and whether this can be related to a helical disposition of the complexes along the column. Second, it was intended to explore the possibility of inducing and tuning supramolecular chirality in chiral and non-chiral mesophases by irradiation with circular polarized light (CPL) as a result of the presence of azobenzene groups.

The complex $M-X12X12$ was CD silent due to the absence of chirality in its chemical structure, whereas $M-X(S)10^*X(S)10^*$ and $M-X(R)10^*X(R)10^*$, bearing chiral alkoxylic chains, displayed non-zero CD spectra (Fig. 6). The appearance of a Cotton effect corresponding to the 1,3,4-oxadiazole chromophore is consistent with helical stacking in the columnar arrangement, as previously reported for structurally similar complexes derived from a melamine core and three V-shaped acids.⁹⁻¹¹ The handedness of this helical arrangement is biased towards a given chiral sense that is determined by the configuration of the stereogenic centre. Thus, the CD spectra of the complexes formed by both enantiomeric acids, $M-X(S)10^*X(S)10^*$ and $M-X(R)10^*X(R)10^*$, present signals of the opposite sign, which indicates enantiomeric helical handedness for both materials. The CD spectra of complexes **M-XA** (see Fig. 7 and S14†) show optical activity for complexes that bear either one or two chiral tails in the acid. The sign of the signal is always positive when one or two (S) 10^* tails are present in the acid and negative when (R) 10^* is present. It was also observed that the presence of a single chiral tail in the V-shaped acids (**XA**) is sufficient to induce CD-active columnar organization. These observations are independent of the chemical nature of the rigid arm in which the tail is located, *i.e.*, either the oxadiazole (X) group or the azobenzene (A) group, as it was also seen for other complexes derived from unsymmetric V-shaped acids.^{11a}

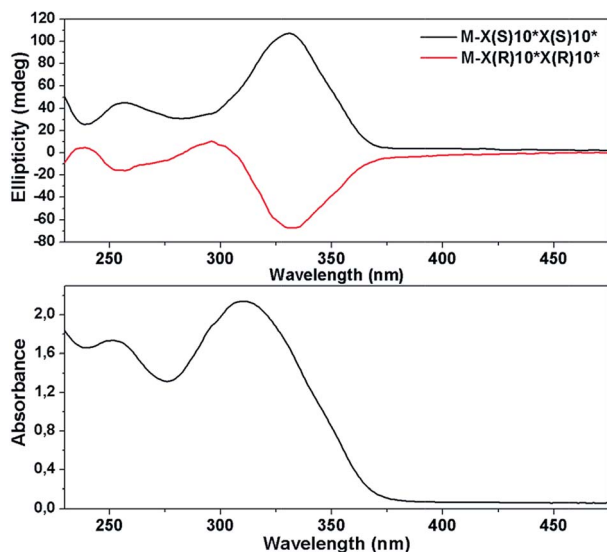


Fig. 6 CD spectra recorded on thin films in the mesophase (25 °C) of the complexes $M-X(S)10^*X(S)10^*$ and $M-X(R)10^*X(R)10^*$.

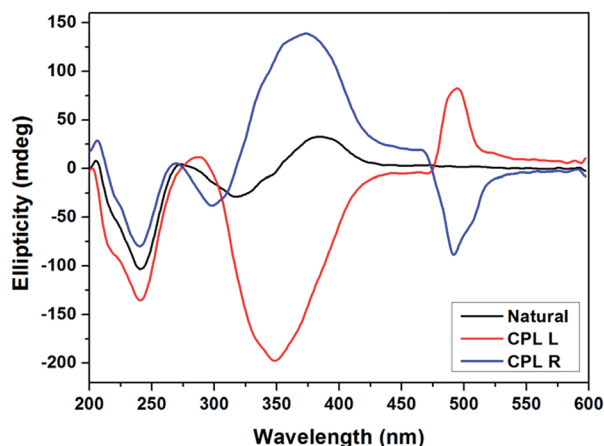


Fig. 7 CD spectra recorded in the mesophase (25 °C) of the complex $M-X(S)10^*A12$.

Experiments aimed at controlling the chirality of the mesophase were performed by irradiating the columnar **M-XA** complexes with CPL. Thin films of the complexes were irradiated with CPL (488 nm, Ar + laser line, 20 mW cm⁻²) at room temperature.

For the complex with only one chiral tail in the 2,5-diphenyl-1,3,4-oxadiazole moiety (**M-X(S)10*A12**), it was possible to amplify its original chirality under right-CPL irradiation and also to induce the opposite signal by irradiating with left-CPL (Fig. 7).

For the complex bearing two chiral tails (**M-A(S)10*X(S)10***) a change was observed in the sign upon irradiation with orthogonal CPLs but an increase in the intensity of the CD signal was not detected (Fig. S14a†). Finally, for the complex that incorporates only one chiral tail in the azo moiety (**M-X12A(S)10***) the CD spectrum showed Cotton effects, but significant changes were not observed upon CPL irradiation (Fig. S14b†). It was

deduced from these experiments that there is a strong dependency of the response of the complexes to CPL with the position of the chiral tail and that the presence of the chiral tail in the azobenzene moiety is less favorable.

In order to corroborate the possibility of not only controlling the chirality of the systems but also of inducing optical activity into an achiral material, complex **M-X12A12** was irradiated with CPL.

The CD spectra corresponding to different irradiation processes are shown in Fig. 8. As expected, the untreated sample did not show a signal due to the absence of chiral tails. Under irradiation with left-handed CPL (l-CPL) and right-handed CPL (r-CPL), non zero CD signals appeared, with opposite sign. The intensity of the signals was dependent on the irradiation time. This means that an amplification of the chirality occurs, and this probably arises from an increase in the population of azobenzene chromophores that absorb light within a helical disposition.

Photophysical properties

The photophysical properties of these complexes, **M-XX** and **M-XA**, were investigated in dilute solutions in dichloromethane and in thin films. The UV-vis absorption and fluorescence spectroscopy data are summarized in Table 2.

For **M-XX**, as shown in Fig. 9, all materials showed similar absorption spectra between 280 and 360 nm, with an intense absorption maximum at 318 nm.

These absorption bands are assigned to $\pi-\pi^*$ transitions of the 1,3,4-oxadiazole heterocyclic due to their high molar absorption coefficients ($\epsilon \sim 20\,000\text{ mol}^{-1}\text{ cm}^{-1}$). All of these compounds displayed strong blue emission in solution (λ_{max} FL 370–530 nm) with intense emission at 418 nm. These complexes showed an excellent photoluminescence quantum yield (ϕ_{FL}) in dichloromethane solution that is quite similar to the value for standard quinine sulfate.²¹

All of the **M-XX** complexes also exhibited fluorescence in thin films. As a consequence of their glassy behaviour, the

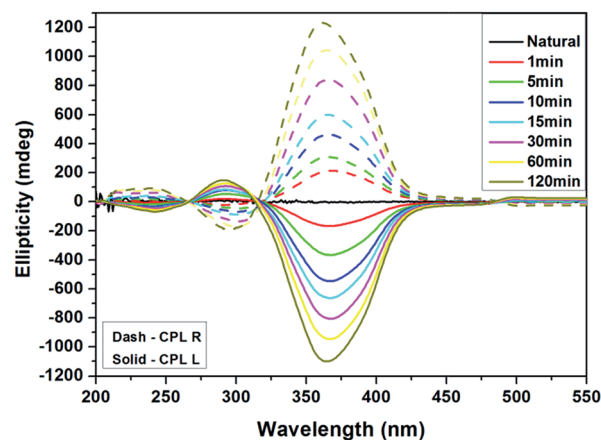


Fig. 8 CD spectra corresponding to successive irradiation on a cast film of complex **M-X12A12**. The irradiation times are given with respect to the previous irradiation step.

Table 2 Optical properties of the complexes M-XX and M-XA

Compound	Abs. λ_{\max} /nm		Fl. λ_{\max} /nm		ϕ_{FL}^c	E_g^d /eV
	Sol. ^a	Film ^b	Sol. ^a	Film ^b		
M-X(S)10*X(S)10*	318	314	423	414	0.97	3.7
M-X(R)10*X(R)10*	318	314	420	414	0.96	3.7
M-X12X12	318	314	423	414	1.00	3.7
M-X(S)10*A(S)10*	326, 368	320	421	—	—	—
M-X(S)10*A12	327, 369	322	420	—	—	—
M-X12A(S)10*	326, 368	317	420	—	—	—
M-X12A12	327, 370	315	424	—	—	—

^a CH₂Cl₂ solution (10⁻⁵ mol L⁻¹). ^b Measurements in the film. ^c Relative to quinine sulfate ($\phi_{\text{FL}} = 0.546$) in CH₂Cl₂. ^d Determined from absorption spectra of the films.

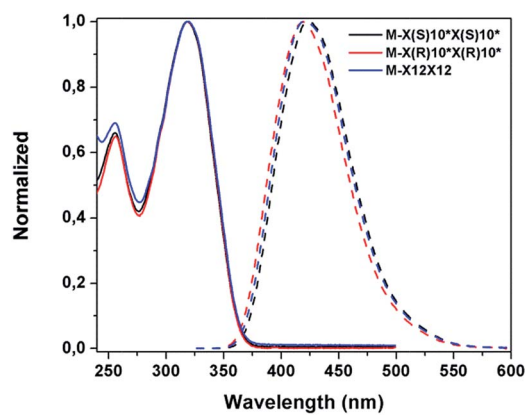


Fig. 9 Absorbance (solid lines) and normalized emission (dashed lines) spectra of the compounds M-XX in solution in CH₂Cl₂ (10⁻⁵ mol L⁻¹).

preparation of the films was easy, and films of high quality were obtained by casting from THF solution on to a quartz plate. Related with the observations from the X-ray experiments commented above, fluorescence spectra were recorded on as-prepared films and on films heated to the isotropic phase followed by slow cooling to ambient temperature (Fig. 10).

As a first observation, it is clear that this class of complex, M-XX, is able to maintain the intrinsic fluorescence from the 1,3,4-oxadiazole in thin films, since absorption and fluorescence profiles similar to those recorded in solution (Fig. 9) were obtained for the films (Fig. 10).

Small differences in the absorbance and fluorescence spectra of the differently treated films were observed. Whereas the absorption maximum is red-shifted for the thermally treated film, the fluorescence maximum is blue-shifted. The effect of re-absorption may change the spectral distribution of their photoluminescence spectra. These can be explained by means of the inner-filter effect which associates the blue shift to a decrease in the film thickness.²² This behaviour should be related to the degree of organization of the material, which is higher for the thermally treated samples (see X-ray diffraction studies).

The optical band gaps (E_g) of all compounds were determined by their corresponding absorption in thin films, using a

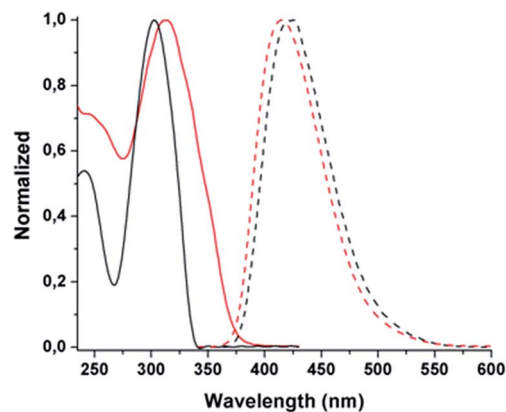


Fig. 10 Normalized absorbance (solid lines) and emission (dashed lines) spectra of the compounds M-X(S)10*X(S)10* in the as-prepared film (black) and mesomorphic glass (red).

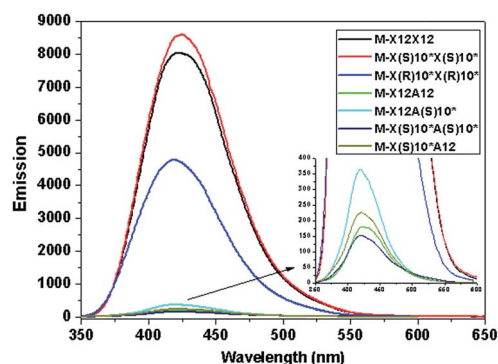


Fig. 11 Emission spectra of the compounds M-XX and M-XA in solution (10⁻⁵ M).²⁵

method reported in the literature.²³ The optical band gaps of these compounds (E_g) varied from 3.6 to 3.7 eV.

The photophysical properties of M-XA complexes were also investigated in CH₂Cl₂ solutions and in thin films. The UV-visible and fluorescence data are summarized in Table 2.

The UV-visible spectra of the complexes in solution showed bands corresponding to the different chromophores present in the molecule, *i.e.*, oxadiazole (X) and azobenzene (A), at around 330 nm and 360 nm, respectively (Fig. S15 in the ESI[†]). These compounds also displayed a weak blue emission at around 420 nm in solution (Fig. 11), but the presence of azobenzene groups led to the loss of fluorescence in thin films.²⁴

Conclusions

In summary, luminescent V-shaped acid derivatives of heterocyclic 1,3,4-oxadiazoles (symmetrical XX and unsymmetrical XA) with different alkyl chains (chiral and non-chiral) were synthesized. These compounds were used to form supramolecular complexes through hydrogen bonding with three acid molecules around the 4-diamino-6-dodecylamino-1,3,5-triazine (M) core. None of the V-shaped acids presented mesomorphism. In contrast, all of the complexes M-XX and M-XA

exhibited liquid crystalline behaviour. **M-XX** presented hexagonal columnar mesomorphism whereas rectangular columnar mesophases were observed for **M-XA** complexes. In any case, the mesomorphic organization remains at room temperature and is frozen below the glass transition in the **M-XX** complexes.

All of the complexes bearing chiral tails derived from citronellol showed optical activity in the mesophase. For azobenzene containing complexes, the possibility of switching reversibly the supramolecular chirality of the material was demonstrated when the chiral tail was located in the oxadiazole arm of the V-shaped acid. Indeed, the optical activity of thin films can be amplified and switched between opposite signs for the complex with only a single chiral tail in the oxadiazole moiety. For the complex with chiral tails in both the oxadiazole and azobenzene arms amplification was not observed but switching between two opposite CD signals could be achieved. In contrast, none of these effects was visible for complexes bearing the chiral tail in the azobenzene moiety. More interestingly, supramolecular chirality is induced in thin films of the achiral complex **M-X12A12**.

M-XX complexes show strong photoluminescence in solution and in the mesophase, as measured at room temperature. However, an almost completely quenched fluorescence is observed for photoresponsive azobenzene containing complexes **M-XA**.

Acknowledgements

We thank the following institutions for financial support: CAPES, CNPq/PRONEX, MINECO (projects MAT38538-CO2-01, MAT2011-27978-CO2-01 and CTQ2012-35692), Gobierno de Aragón (project E04) and the EU (FEDER and FSE founding). Thanks are due to: Nuclear Magnetic Resonance, Mass Spectrometry, Elemental Analysis and Thermal Analysis Services of the CEQMA, Universidad de Zaragoza-CSIC (Spain).

Notes and references

- (a) E.-K. Fleischmann and R. Zentel, *Angew. Chem., Int. Ed.*, 2013, **52**, 8810–8827; (b) D. J. Broer, C. M. W. Bastiaansen, M. G. Debije and A. P. H. J. Schenning, *Angew. Chem., Int. Ed.*, 2012, **51**, 7102–7109; (c) T. Kato and K. Tanabe, *Chem. Lett.*, 2009, **38**, 634–639.
- (a) K. Tschierske, *Angew. Chem., Int. Ed.*, 2013, **52**, 8828–8878; (b) R. J. Bushby and K. Kawata, *Liq. Cryst.*, 2011, **38**, 1415–1426; (c) B. R. Kaafarani, *Chem. Mater.*, 2011, **23**, 378–396; (d) T. Kato, T. Yasuda, Y. Kamikawa and M. Yoshio, *Chem. Commun.*, 2009, 729–739; (e) S. Laschat, A. Baro, N. Steinke, F. Giesselmann, C. Hägele, G. Scalia, R. Judele, E. Kapatsina, S. Sauer, A. Schreivogel and M. Tosoni, *Angew. Chem., Int. Ed.*, 2007, **46**, 4832–4887; (f) S. Laschat, A. Baro, N. Steinke, F. Giesselmann, C. Hägele, G. Scalia, R. Judele, E. Kapatsina, S. Sauer, A. Schreivogel and M. Tosoni, *Angew. Chem., Int. Ed.*, 2007, **46**, 4832–4887; (g) S. Sergeev, W. Pisula and Y. H. Geerts, *Chem. Soc. Rev.*, 2007, **36**, 1902–1929.
- (a) J. Shu, D. Dudenko, M. Esmaili, J. H. Park, S. R. Puniredd, J. Y. Chang, D. W. Breiby, W. Pisula and M. R. Hansen, *J. Am. Chem. Soc.*, 2013, **135**, 11075–11086; (b) C. Domínguez, B. Heinrich, B. Donnio, S. Coco and P. Espinet, *Chem.–Eur. J.*, 2013, **19**, 5988–5995; D. Tsiourvas and M. Arkas, *Polymer*, 2013, **54**, 1114–1122; (c) S. Castelar, J. Barberá, M. Marcos, P. Romero, J.-L. Serrano, A. Golemme and R. Termine, *J. Mater. Chem. C*, 2013, **1**, 7321–7332; (d) S. Moyano, J. Barbera, B. E. Diosdado, J. L. Serrano, A. Elduque and R. Gimenez, *J. Mater. Chem. C*, 2013, **1**, 3119–3128; (e) S. J. Lee, J. Lee, S. W. Lee, J. H. Lee and J. Y. Jho, *J. Ind. Eng. Chem.*, 2012, **18**, 767–774; (f) B. Bai, C. Zhao, H. Wang, X. Ran, D. Wang and M. Li, *Mater. Chem. Phys.*, 2012, **133**, 232–238.
- F. Vera, J. L. Serrano and T. Sierra, *Chem. Soc. Rev.*, 2009, **38**, 781–796.
- (a) Y. Shirota and H. Kageyama, *Chem. Rev.*, 2007, **107**, 953–1010; (b) M. Sawamura, K. Kawai, Y. Matusuo, K. Kanie and T. Kato, *Nature*, 2002, **419**, 702–705; (c) I. Seguy, P. Jolinat, P. Destruel and R. Mamy, *J. Appl. Phys.*, 2001, **89**, 5442–5448; (d) A. M. Van de Craats, N. Stutzmann, M. M. Nielsen and M. Watson, *Adv. Mater.*, 2003, **15**, 495–499.
- (a) T. Kato, T. Matsuoka, M. Nishii, Y. Kamikawa, K. Kanie, T. Nishimura, E. Yashima and S. Ujiie, *Angew. Chem., Int. Ed.*, 2004, **43**, 1969–1972; (b) Z. Tomovic, J. van Dongen, S. J. George, H. Xu, W. Pisula, P. Leclere, M. M. J. Smulders, S. De Feyter, E. W. Meijer and A. P. H. J. Schenning, *J. Am. Chem. Soc.*, 2007, **129**, 16190–16196; (c) M. Peterca, M. R. Imam, C.-H. Ahn, V. S. K. Balagurusamy, D. A. Wilson, B. M. Rosen and V. Percec, *J. Am. Chem. Soc.*, 2011, **133**, 2311–2328.
- (a) T. Ishi-i, R. Kuwahara, A. Takata, Y. Jeong, K. Sakurai and S. Mataka, *Chem.–Eur. J.*, 2006, **12**, 763; (b) M. Peterca, V. Percec, A. E. Dulcey, S. Nummelin, S. Korey, M. Ilies and P. A. Heiney, *J. Am. Chem. Soc.*, 2006, **128**, 6713; (c) D. Franke, M. Vos, M. Antonietti, N. A. J. M. Sommerdijk and C. F. J. Faul, *Chem. Mater.*, 2006, **18**, 1839; (d) J. van Gestel, A. R. A. Palmans, B. Titulaer, J. A. J. M. Vekemans and E. W. Meijer, *J. Am. Chem. Soc.*, 2005, **127**, 5490; (e) J. Barberá, L. Puig, P. Romero, J. L. Serrano and T. Sierra, *J. Am. Chem. Soc.*, 2005, **127**, 458; (f) T. Kato, T. Matsuoka, M. Nishii, Y. Kamikawa, K. Kanie, T. Nishimura, E. Yashima and S. Ujiie, *Angew. Chem.*, 2004, **116**, 2003; *Angew. Chem., Int. Ed.*, 2004, **43**, 1969; (g) M. L. Bushey, T. Q. Nguyen, W. Zhang, D. Horoszewski and C. Nuckolls, *Angew. Chem.*, 2004, **116**, 5562; *Angew. Chem., Int. Ed.*, 2004, **43**, 5446; (h) J. L. Serrano and T. Sierra, *Coord. Chem. Rev.*, 2003, **242**, 73. For a general survey on hydrogen-bonded liquid crystals, see: (i) T. Kato, N. Mizoshita and K. Kishimoto, *Angew. Chem.*, 2006, **118**, 44; *Angew. Chem., Int. Ed.*, 2006, **45**, 38.
- R. M. Tejedor, L. Oriol, J. L. Serrano and T. Sierra, *J. Mater. Chem.*, 2008, **18**, 2899–2908.
- J. Barberá, L. Puig, P. Romero, J. L. Serrano and T. Sierra, *J. Am. Chem. Soc.*, 2006, **128**, 4487–4492.
- A. Vieira, H. Gallardo, J. Barberá, P. Romero, J. L. Serrano and T. Sierra, *J. Mater. Chem.*, 2011, **21**, 5916–5922.

- 11 (a) F. Vera, J. L. Serrano, M. P. de Santo, R. Barberi, M. B. Ros and T. Sierra, *J. Mater. Chem.*, 2012, **22**, 18025–18032; (b) J. R. Avilés Moreno, J. J. López González, F. Partal Ureña, F. Vera, M. B. Ros and T. Sierra, *J. Phys. Chem. B*, 2012, **116**, 5090–5096; (c) F. Vera, R. M. Tejedor, P. Romero, J. Barberá, M. B. Ros, J. L. Serrano and T. Sierra, *Angew. Chem., Int. Ed.*, 2007, **46**, 1873–1877.
- 12 Y. Cao, X. Chai, S. Chen, Y. Jiang, W. Yang, R. Lu, Y. Ren, M. Blanchard-Desce, T. Li and J. Lehn, *Synth. Met.*, 1995, **71**, 1733–1734.
- 13 H. Gallardo, R. Magnago and A. J. Bortoluzzi, *Liq. Cryst.*, 2001, **28**, 1343–1352.
- 14 R. Cristiano, A. A. Vieira, F. Ely and H. Gallardo, *Liq. Cryst.*, 2006, **33**, 381–390.
- 15 F. Vera, P. Romero, J. Barberá, M. B. Ros, J. L. Serrano and T. Sierra, *Angew. Chem., Int. Ed.*, 2010, **49**, 4910–4914.
- 16 (a) E. Beltrán, E. Cavero, J. Barberá, J. L. Serrano, A. Elduque and R. Giménez, *Chem.–Eur. J.*, 2009, **15**, 9017–9023; (b) J. Barberá, L. Puig, P. Romero, J. L. Serrano and T. Sierra, *Chem. Mater.*, 2005, **17**, 3763–3771.
- 17 The absence of some reflections, such as (11) and (20) is not infrequent in the X-ray patterns of hexagonal columnar mesophases and it is due to a minimum in the structure factor, which precludes the observation of peaks at the corresponding diffraction angles. See: (a) W. Pisula, Z. Tomovic, Ch. Simpson, M. Kastler, T. Pakula and K. Mullen, *Chem. Mater.*, 2005, **17**, 4296–4303; (b) B. Kohne, K. Praefcke and W. Stephan, *Chimia*, 1986, **40**, 14; (c) H. Strzelecka, C. Jallabert, M. Veber, P. Davidson and A. M. Levelut, *Mol. Cryst. Liq. Cryst.*, 1988, **161**, 395; (d) J. Barberá, C. Cativiela, J. L. Serrano and M. M. Zurbano, *Adv. Mater.*, 1991, **3**, 602; (e) J.-H. Olivier, F. Camerel, J. Barberá, P. Retailleau and R. Ziessel, *Chem.–Eur. J.*, 2009, **15**, 8163; (f) F. Camerel, G. Ulrich, J. Barberá and R. Ziessel, *Chem.–Eur. J.*, 2007, **13**, 2189.
- 18 G. S. Hartley, *Nature*, 1937, **140**, 281.
- 19 S.-W. Choi, S. Kawauchi, N. Y. Ha and H. Takezoe, *Phys. Chem. Chem. Phys.*, 2007, **9**, 3671–3682.
- 20 G. Gottarelli, S. Lena, S. Masiero, S. Pieraccini and G. P. Spada, *Chirality*, 2008, **20**, 471–485.
- 21 S. R. Meech and D. Phillips, *J. Photochem.*, 1983, **23**, 193.
- 22 N. F. Marcelo, A. A. Vieira, R. Cristiano, H. Gallardo and I. H. Bechtold, *Synth. Met.*, 2009, **159**, 675.
- 23 A. Joshi, M. O. Manasreh, E. A. Davis and B. D. Weaver, *Appl. Phys. Lett.*, 2006, **89**, 111907–111910.
- 24 B. Valeur, *Molecular Fluorescence, Principles and Applications*, Wiley-VCH, Weinheim, 2002.
- 25 Solution concentrations: **M-X12X12**, 4.0×10^{-5} M; **M-X(S)10*X(S)10***, 4.5×10^{-5} M; **M-X(R)10*X(R)10***, 3.0×10^{-5} M; **M-X12A12**, 3.4×10^{-5} M; **M-X12A(S)10***, 4.2×10^{-5} M; **M-X(S)10*A(S)10***, 3.0×10^{-5} M; **M-X(S)10*A12**, 4.1×10^{-5} M.